

Detailed observations of the phytoplankton spring bloom in the stratifying central North Sea

by Hans van Haren¹, David K. Mills² and Lambertus P. M. J. Wetsteyn³

ABSTRACT

Analysis of detailed time series of bio-optical and temperature data from the North Sea supports the view that a minimum level of turbulence is a prerequisite for the onset and maintenance of the phytoplankton spring bloom in shelf seas, which distinguishes these seas from the open ocean. The start of the spring bloom, primarily diatoms, is controlled by the light regime, while its progress is predominantly dependent upon episodic turbulence input following short periods of stratification, which allow the resuspension of a fast sinking ($50\text{--}200\text{ m day}^{-1}$) phytoplankton community from the bottom mixing layer. A relationship between turbulence and the vertical distribution of phytoplankton is proposed which is found at synoptic time scales and on time scales of a day and less.

Throughout the spring bloom, algal biomass is either equally distributed through the water column or concentrated in the bottom mixing layer. Growth can only be sustained in the near-surface layer during periods of substantial turbulence input. The establishment of semi-permanent seasonal stratification causes an almost complete reduction in near-surface biomass and a concomitant increase in biomass in the bottom mixing layer which subsequently acts as a source for occasional increased near-surface biomass until early summer.

1. Introduction

Life in shelf seas is abundant when compared to the ocean. High levels of primary production and phytoplankton biomass reflect a favorable environment in terms of light and the supply of inorganic nutrients. However, it has been recognized by Riley *et al.* (1949), Munk and Riley (1952) and Margalef (1978) that the most important factor controlling phytoplankton is its movement through the water column, by sedimentation or turbulence and advection. Such processes especially determine the distinction in phytoplankton biomass between shelf seas and the ocean, which is most pronounced during bloom periods in spring and late summer (Riegman *et al.*, 1993).

Nevertheless, the timing of the marine phytoplankton spring bloom is held to be primarily controlled by the subsurface light regime (Tett, 1990). As light decreases exponentially with depth in the sea, the influence of turbulent mixing becomes important in

1. Netherlands Institute for Sea Research (NIOZ), P. O. Box 59, 1790 AB Den Burg, The Netherlands.

2. Centre for Environment, Fisheries and Aquaculture Sciences (CEFAS), Lowestoft, Suffolk, United Kingdom, NR33 OHT.

3. National Institute for Coastal and Marine Management (RIKZ), P. O. Box 8039, 4330 EA Middelburg, The Netherlands.

this viewpoint because algae will experience a range of irradiance levels down to the critical limit for growth as they cycle through the water column. Then, an additional problem is encountered when algae sink relatively fast out of the euphotic zone. Consequently, the subtle balance between the level of turbulence and the sinking rate of algae has generated an ongoing debate.

When sinking rates are small ($<1 \text{ m day}^{-1}$) turbulence entirely determines the time spent at a certain depth. This is the prevailing situation for small algae and in the ocean, where fast sinking rates would cause definite loss from the euphotic zone, as has been shown by Woods and Onken (1982). Models using such low sinking rates have been developed for shelf seas, to explain the summer maximum at the pycnocline (Sharples and Tett, 1994), and for estuaries, to explain the apparent spring bloom occurrence at neap tides (Cloern, 1991). In essence, these models may hold during the summer for algae, such as dinoflagellates (Smayda, 1970), but probably cannot explain the spring bloom in shelf seas.

These blooms primarily consist of diatoms, and their sinking rates are reported to vary between $0.1\text{--}30 \text{ m day}^{-1}$ (Smayda, 1970) and greater than 70 m day^{-1} (Passow, 1991). Theoretically, it has been shown that such large algae need to sink relatively fast for sufficient nutrient uptake (Munk and Riley, 1952). Therefore, we postulate that they can only exist in shallow seas and estuaries, where the level of turbulence is relatively high and the bottom is not too far below the euphotic zone, which prevents final loss following episodic events of large turbulence input.

Due to vertical mixing by turbulence, the nutrients providing bottom boundary layer may be “coupled” with the euphotic zone. Turbulence is generated at the bottom by (tidal) currents through friction and near the surface by wind stress, breaking waves and free convection due to (night-time) cooling, and is therefore strongly time dependent. For instance, turbulence generated near the sea surface has to overcome the stabilizing effect of heat input to be effective for mixing, and will show a daily cycle (Taylor and Stephens, 1993; Brainerd and Gregg, 1995). This stabilization of the water column can be modeled by a reduction of scales over which turbulence acts (Tennekes and Lumley, 1972; Niiler and Kraus, 1977). As a result, algae cycle different parts of the water column and at different time scales during stratifying and mixing periods (Lewis *et al.*, 1984; Denman and Gargett, 1988; Taylor and Stephens, 1993).

Here we present the first part of year long field data obtained during the Integrated North Sea Programme (INP) to study the effects of mixing on the variations of phytoplankton abundance with time. The main body of data comes from an array of hourly sampling fluorometers, light meters, temperature sensors and current meters that were moored in the central North Sea in 1994. The key points to be addressed in this paper are the distribution of algal biomass through the water column during and after the spring bloom, their relation to (inferred) turbulence level variations and the timing of the spring bloom in relation to stratification rate and light levels. Special attention is given to the (sub-)daily variations of fluorescence.

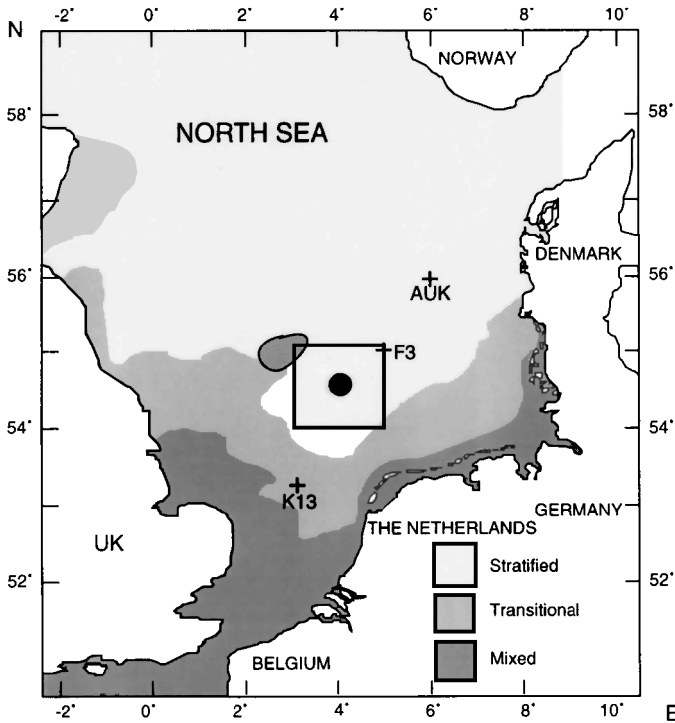


Figure 1. Map of the INP study area (rectangle), the mooring site (●) and the platforms K13, F3 and AUK where meteorological data were sampled. The extent of summer stratification in this region is also shown (redrawn from Pingree and Griffiths, 1978).

2. Data acquisition, calibration and analysis procedures

The INP mooring site is located in the central North Sea, Oyster Grounds, at $54^{\circ} 25'N$ and $04^{\circ} 02'E$, where the water depth is about 45 m (Fig. 1). The horizontal currents are dominated by the semidiurnal tide, with the major axis directed east-west and amplitudes varying between $0.2\text{--}0.3\text{ ms}^{-1}$. The bottom mixing layer extends to about 25 m above the bottom (Maas and van Haren, 1987). Consequently, the surface and bottom mixing layers overlap when the atmospherically induced turbulence reaches deeper than 20 m. As a result, the location is well within the region of seasonal stratification (Pingree and Griffiths, 1978), and generally away from frontal zones, although, occasionally, passing frontal meanders could not be avoided during the study (cf Section 2c and van Aken *et al.*, 1987). CTD observations show that stratification, when present, is thermally induced and no indications have been found for any salinity contributions to its onset, as has been suggested by van Aken (1986).

Moorings were deployed between January and June 1994 with different arrays of instruments (Table 1). During the full period of study the water temperature and, hence, stratification rate were monitored from surface to bottom using thermistor strings holding

Table 1. Summary of mooring instrumentation and accuracies. The format of useful data return (under header 1994) is number of instruments (**bold**): months of good operation (3 = March etc). The mooring site has been occupied between months 1–6, 1994.

Instrument type	Manufacturer	1994	Standard depths	Accuracy after calibrations
current meter	NBA/Aanderaa	4–5 :1–6	12, 23, 40, 42, 44 m	0.02 ms ⁻¹ , 1.5 °TN, 0.02 °C
meteo buoy	Aanderaa	1 :3, 5–6	2 mas*	0.2 ms ⁻¹ , <5 °, 10 W m ⁻² , 0.1 °C#
thermistor string†	Aanderaa	1–3 :1–6	2–43 m every 2 m	0.02 °C
PAR sensor	Licor/Leica	1 :1–2, 2 :3–6	2 mas, 11, 23 m	<5 µE m ⁻² s ⁻¹
fluorometer	Chelsea Instr.	1 :1–6, 2 :3–4	11, 23 m	0.1 mg m ⁻³
transmissometer	WS-Oceans‡	1 :1–6 1–6	12 m	0.03 m ⁻¹

*: mas = m above the sea surface.

#: Accuracies for wind speed, wind direction, net radiation, air temperature.

†: All current meters and several other instruments were equipped with thermistors. Data from these sensors are used during (occasional) thermistor string failure.

‡: We bought our first transmissometer directly from the developer, UNCW Bangor (UK), before they licensed WS-Oceans for further production.

11 thermistors at 2 m intervals. The upper thermistor string was suspended from a surface buoy. All other instruments recording data on physical and bio-optical parameters were deployed beneath a subsurface buoy at a depth of about 10 m to avoid the effects of severe wind and wave action, typical for the North Sea, albeit preventing the monitoring of the first 11 m of the water column. In general, the data return was acceptable with little evidence of fouling of optical instruments during the study period.

The instruments were set to sample data at least hourly and data from faster sampling instruments like current meters and thermistor strings were hourly filtered prior to analysis. The fluorometers recorded ensembles (and their standard deviations) of 60 samples obtained within 180 s, every hour. As a result, each fluorescence value recorded constitutes a reduction of instrumental noise and a smoothed estimate from a patch of phytoplankton across a typical horizontal scale of about 40 m, which is advected past the sensor by the (tidal) current.

At least once a month the mooring site was visited by the *R. V. Pelagia* for instrument servicing and additional sampling for calibration and hydrographic purposes. About every three weeks the *R. V. Holland* sampled data (a.o. on extracted chlorophyll-*a* and species composition) on their monitoring transect across the INP site. No experiments were performed on growth and respiration rates. The atmospheric conditions were extracted from data from three fixed platforms, K13, F3 and AUK, which were located 100–200 km from the mooring site (Fig. 1). From March 1994 onwards a meteorological buoy was moored at the INP site.

In addition to the net radiation sensor on the meteorological buoy, quantum cosine

response sensors, measuring PAR (Photosynthetic Active Radiation; 400–700 nm) irradiance, were deployed above the sea surface and at 11 and 23 m depth (generally 0.5 m below a fluorometer). In spring these depths represent more or less the surface and bottom mixing layers, respectively. During the entire spring bloom period (to be defined in Section 3) the daily averaged PAR at 23 m remained below the canonical level of $6.3 \mu\text{E m}^{-2} \text{s}^{-1}$ ($\approx 1.5 \text{ W m}^{-2}$ in the 400–700 nm band), which is the minimum considered necessary for growth (Tett, 1990). Under the assumption of an exponential decrease of PAR with depth, the irradiance attenuation coefficient k was computed between each pair of quantum sensors.

A transmissometer moored at 12 m depth provided data on the beam attenuation coefficient (b) in a 30 nm optical band around 670 nm. In general, a linear relationship was found between daily averaged b and the irradiance attenuation coefficient k , according to $k \approx 0.26 b + 0.04$, which is in close agreement with results by Mills *et al.* (1994), and b and k are equally used to describe daily averaged “vertical light attenuation.”

a. Calibrations

In addition to manufacturer’s calibrations of all moored sensors, laboratory calibrations were performed on the compasses of the current meters and on all under-water temperature sensors (cf. Table 1 for the resulting accuracies). Our rotating aluminium frame for the former calibration has an accuracy of positioning better than 0.5° and the thermostatic bath used for temperature calibrations can be held stable to within 5 mK. As a result, relative accuracies could be achieved that approached the resolution of the sensors.

Special calibrational attention was given to the fluorometers, because varying physiological and environmental factors affect the fluorescence emission coefficient, (E ; *in vivo* fluorescence normalized to unit chlorophyll concentration). Factors affecting the E and, hence, fluorometer data, include species composition (Pingree and Harris, 1988; Prézélin and Ley, 1980), and ambient light field (Lewis *et al.*, 1984; Mills and Tett, 1990). A reduction in E is reported to occur when $\text{PAR} > 250\text{--}600 \mu\text{E m}^{-2} \text{s}^{-1}$ and the time of exposure is longer than 1 hour (Lewis *et al.*, 1984). Although we cannot rule out changes in species composition the large diatom *Guinardia flaccida* appeared to dominate the phytoplankton during the major part of the study.

To investigate some of the effects of species composition on E , the fluorometers were calibrated twice in the laboratory. During the first calibration a culture of diatoms (*Ditylum* sp.) was used and during the second a culture of dinoflagellates (*Amphidinium* sp.), which are representative of the typical spring and summer algae species, respectively. The resulting linear fits (Fig. 2a) between HPLC determined chlorophyll-*a* and fluorometer data were different for each individual instrument and much less so for each culture. The diatom calibration of each instrument was used on the spring period data.

The validity of the laboratory calibration was checked by comparing the fluorometer data adjusted after the laboratory calibration (“raw chlorophyll data”) with extracted chlorophyll-*a* measured in water samples collected within 1 km horizontally from the

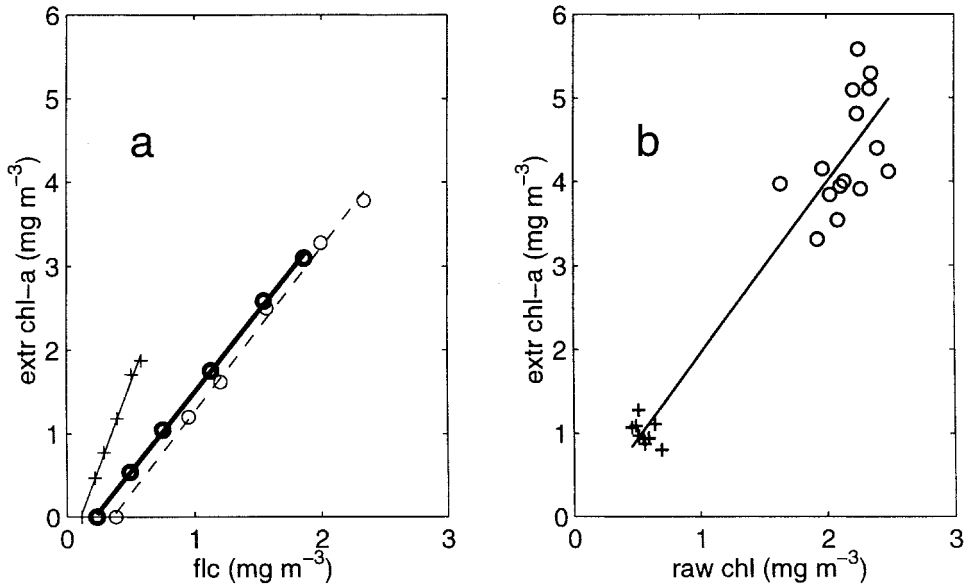


Figure 2. Fluorometer calibrations. (a) Laboratory calibrations of two fluorometers (Chelsea Inst. MKIII ser. no. 001 (○) and 007 (+)) using two cultures, diatoms (*Ditylum* sp., solid lines) and dinoflagellates (*Amphidinium* sp., dashed line). Uncalibrated fluorescence data (flc) are plotted against extracted chlorophyll-*a*. The thick line calibration is used to generate "raw chlorophyll data." (b) Scatter plot between laboratory calibrated fluorometer data ("raw chl") and extracted chlorophyll-*a* from *in situ* water samples taken during winter (+) and early spring (○).

mooring location and within 5 m vertically from the depth of each fluorometer. Known volumes were filtered through Whatman GF/C filters and chlorophyll-*a* determined by HPLC. A reasonably linear fit was found between the "raw chlorophyll data" and the extracted winter and spring chlorophyll-*a* data (Fig. 2b), but the slope is greater than one. We conclude that although laboratory calibrations may be helpful in determining the linearity of response of a fluorometer, field calibrations remain necessary for determining absolute chlorophyll values from fluorometer data. The scatter in the field calibration data is larger than in the laboratory calibration data and may be attributed to several reasons.

Sources of variability include possible differences in extracted chlorophyll concentration in the viewing area of the fluorometer and the water sample. Further sources of variability include differences between field and laboratory populations in terms of species composition and in their photoadaptive state. However, diatoms were shown to be dominant in the field and were also used in the laboratory calibration and, as we demonstrate subsequently (Section 4), photoinhibition can be ruled out.

b. Monitoring turbulence variability

Knowledge about the variations with time and depth of the amount of turbulence is a prerequisite in a study on vertical exchange of heat, dissolved and suspended matter. We

have not measured turbulence directly, but we will represent it by using variations with time of observed vertical temperature differences, which indicate the result of active mixing outside frontal regions. Ideally, one would rely on measurements of thermal overturning scales to estimate the mixing layer depth and the rate of mixing (Thorpe, 1977), but in practice this is difficult with CTD or moored (standard) thermistor string (Brainerd and Gregg, 1995). We use their observations that a mixing layer may be determined by very small vertical temperature differences (e.g. $\Delta T < 0.01^\circ\text{C}$) and that a fixed value of ΔT cannot be related to a certain level of turbulence. Here we assume that turbulence has been (instantaneously) reduced as soon as $\Delta T > 0.01^\circ\text{C}$, for ΔT between the surface (2 m depth) and deeper in the water column (either 22 m depth or the bottom).

After some tests it appeared that the use of the directly measured parameter ΔT resembles closely the more physical parameter on the stability of the water column, i.e. the integral amount of potential energy of the water column (e.g. van Aken, 1986),

$$V(t) = \int_{-H}^0 (\rho - \langle \rho \rangle) g z \, dz \propto -\Delta T;$$

where $\langle \rho \rangle = 1/H \int_{-H}^0 \rho \, dz$, H the water depth, $\rho(z, t)$ the density and g the acceleration of gravity.

Alternatively, the amount of turbulence generated may be inferred from current meter and atmospheric data using bulk formulae (Niiler and Kraus, 1977; van Aken, 1986). Here, we refrain from using these formulae other than in a qualitative sense, because they are generally valid for quantities averaged over time scales of a day or so, which is too long for the variations studied here. It is beyond the scope of this paper to incorporate such data in a coupled physical-biological vertical mixing model and to tune the results with observations (cf. Sharples and Tett, 1994; Ruudij *et al.*, 1997).

Qualitatively, we keep in mind that near the sea surface turbulence is produced when the heat fluxes are positive (free convection) and by the wind. Near the sea bed turbulence is produced by friction of currents and waves. Our hypothesized agreement between heat and biomass variability with time due to vertical turbulent exchange reads as follows.

The balance for the rate of heat change at depth $-z$ is assumed as,

$$\frac{\partial \bar{T}}{\partial t} = \bar{K} \bar{I} / \rho c_p - \frac{\partial \overline{w'T'}}{\partial z}; \quad -\overline{w'T'}|_0 = Q_t / \rho c_p, \quad (1)$$

where all variables are a function of (z, t) , the overbar denotes averaging over a certain period (hourly, daily), the prime the fluctuations about the mean, w the vertical velocity component, ρ the density, c_p the heat capacity of water and I is the penetrative part (γ) of solar radiation ($I = \gamma Q_0 e^{kz}$). Q_t is proportional to the total heat flux across the sea surface.

The last term in (1) denotes the divergence of vertical turbulent heat flux, which may be parameterized by $\overline{w'T'} = -\bar{K} \partial \bar{T} / \partial z$, where the turbulent eddy diffusivity coefficient K is proportional to a typical vertical overturning scale ($K \sim 1/\Delta T$ the thermocline thickness, or the water depth) and the rate of turbulence production (Tennekes and Lumley, 1972). In

principle, the acceptance of the above parameterization may lead to quantitative estimates for turbulent exchange using the observed (bulk) data in (1). However, over the (subdaily) time scales we are interested in here, attempts to yield realistic results failed, presumably because the resolution and accuracy of the temperature sensors were insufficient to resolve the weak local derivatives and gradients.

Equivalently, the equation for the chlorophyll (and therefore phytoplankton biomass) concentration C is written as,

$$\frac{\partial \bar{C}}{\partial t} - \bar{w}_s \frac{\partial \bar{C}}{\partial z} = \bar{\mu}(\text{PAR}, N) \bar{C} - \frac{\partial \overline{w' C'}}{\partial z}, \quad (2)$$

where the net production is given by the first term on the right-hand side, which depends on PAR and nutrient concentration N (Sharples and Tett, 1994), and which includes respiratory and grazing losses. Like all other parameters, the sinking velocity magnitude w_s is a function of (z, t) to allow for varying (species or aggregating related) sinking rates. The rate of change with time may differ strongly between C and T , when heating is dominated by direct insolation rather than turbulent exchange and when net production is limited by nutrients, grazing or respiration. The redistribution by turbulence relies on the diffusivity coefficient K as before. The obvious difference between (1) and (2) is the inclusion of a vertical “advection” term in (2), which we consider not small in our case.

c. Advection

Turbulence is not the only means to transport matter and spatially inhomogeneous phytoplankton distributions may be advected past moored sensors by currents. However, terms describing advection other than due to sinking are not considered in (1) and (2). If we assume that on the time scales of one hour and longer, surface wave action and (night-time) free convection manifest themselves as “turbulence,” the vertical advection term is generally weak. An upper limit would be found in up- or downwelling regions, but even there, typical vertical current velocity amplitudes are found of $O(10^{-4} \text{ m s}^{-1})$ or 10 m day^{-1} ; van Haren and Joordens, 1990). As the possible variability of phytoplankton over small horizontal scales of $O(10 \text{ m})$ has been smoothed by the sampling strategy, horizontal advection manifests itself predominantly in the most energetic frequency bands, which are the semi-diurnal tidal and synoptic (wind-driven) bands in our area, and not the diurnal band.

Evidence of horizontal advection has been found from inspection of the tidal and synoptic bands from the time series in association with data collected during a quasi-synoptic survey at stations about 3 km apart. As an example we show temperature data from sensors attached to an accidentally freely drifting buoy with data from moored sensors (Fig. 3). However, horizontal advection only occurred during isolated periods of a few days and is clearly visible when present (e.g. between days 89–92 and 100–105 in Figure 3b, when tidal advection is apparent, which shows up in data from a fixed mooring and not in data from a quasi-Lagrangian drifter (van Haren and Maas, 1987)). Furthermore,

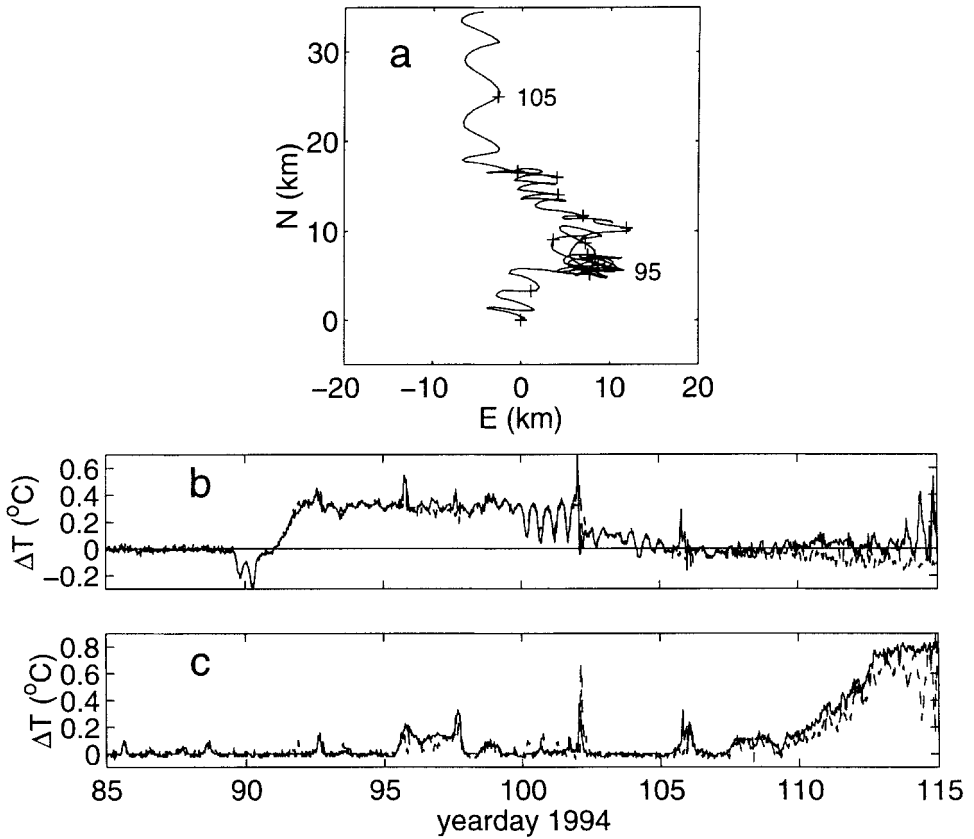


Figure 3. The influence of horizontal advection on temperature observations as inferred from the comparison of data from a fixed mooring and from a buoy, which accidentally broke lose from the mooring site at (0,0). (a) Likely relative displacement of the buoy from the mooring site at (0,0), as inferred from local current data, with midnight marks (+) and day numbers. The buoy was retrieved at $55^{\circ} 00'N$, $03^{\circ} 50'E$ at day 121. The progressive vector diagram reaches to within 5 km from that position at that day. (b) Temperature differences between the fixed mooring and the buoy at 12 (solid line) and 23 m depth (dashed line). (c) Vertical temperature differences between 12 and 23 m observed at the buoy (solid line) and at the fixed mooring (dashed line). Time is given in yeardays, according to the convention that January 1, 12.00 UTC = yearday 0.5.

it appeared that differential horizontal advection was relatively weak for both temperature and biomass during most of the period of measurements so that we basically consider vertical differences in our analysis (Fig. 3c, in which no tidal signal is found).

3. General aspects of the observed spring bloom

During the winter, light levels are generally limiting for phytoplankton growth due to low surface solar irradiance and elevated values of the vertical attenuation coefficient

(occasionally, $k \approx 0.5\text{--}1\text{ m}^{-1}$ during stormy weather periods, presumably due to increased levels of bubbles near the surface and suspended matter concentrations near the bottom). The observed over-winter nutrient concentrations are $6 \pm 1\ \mu\text{M}$ (NO_x) and $2.5 \pm 0.5\ \mu\text{M}$ (Si), which potentially allow for a phytoplankton population of roughly $5\text{--}10\ \text{mg m}^{-3}$ in chlorophyll units, using some rule of thumb Redfield and C/chl ratios. Such a population may consist mainly of diatoms, as a nonlimiting value of $\text{N/Si} \approx 2$ has been observed for freshwater diatoms (Healey, 1973) and we cannot think of any reason why such value would be different for North Sea diatoms. Given the uncertainties of different populations requiring different amounts of nutrients, our winter values correspond well with the ratio quoted.

The observed winter values of chlorophyll concentrations are about $0.5 \pm 0.1\ \text{mg m}^{-3}$. We define the start of the spring bloom⁴ when the daily averaged chlorophyll concentration (as measured by *in situ* fluorescence at 11 m depth) exceeds the winter value. This occurs at the end of February (day 56; Fig. 4), when the daily averaged PAR at 11 m and the daily mean PAR averaged over the whole water column just exceed the minimum value for growth. During the initial period of steady growth the irradiance attenuation coefficient decreases, although the wind speeds remain roughly constant, but PAR at 11 m barely exceeds the critical level.

The chlorophyll level suddenly increases further from 1.5 to $2\ \text{mg m}^{-3}$ near day 72, while a storm passes by, k increases to winter values and (local) light levels are below threshold. Hence, one questions whether this sudden increase in chlorophyll may be attributed to actual growth, to horizontal advection or to increased vertical mixing following sinking. It may indicate however, a transition from a system which contains small algae to a (nonoceanic) system that also contains meso-algae, which was confirmed by comparison of the species compositions of the samples taken at days 11 and 69. A value of chlorophyll-*a* $\approx 1\ \text{mg m}^{-3}$ has been reported for this transition (Riegman *et al.*, 1993).

From day 72 onwards the chlorophyll levels observed at 11 m show an irregular and fluctuating pattern, independent of the daily mean PAR at 11 m, which increases slowly with time. In fact, an inverse relationship between chlorophyll and PAR appears at times (e.g. between days 83–90 and 96–110). Unless one attributes phytoplankton growth to a relationship between PAR and chlorophyll with a phase delay of about 1–3 days, our data suggest that measured PAR reflects the amount of biomass in the water column, not related to growth. Between days 72 and 90 the net increase in chlorophyll is negligible and horizontal advection seems dominant for most parameters, including temperature and nutrients, as has been inferred from the tidal and subtidal variabilities and from their vertical consistency in records like presented in Figure 5a. (to be discussed in Section 4a).

The spring bloom declines in the near-surface layer, with chlorophyll decreasing from its maximum value of the year (of about $6.5\ \text{mg m}^{-3}$, consistent with our rough estimate based on the winter nutrients input, and in agreement with values reported earlier for the central

4. Throughout the paper we will use “bloom” for chlorophyll concentrations above the winter level, without considering the level of growth.

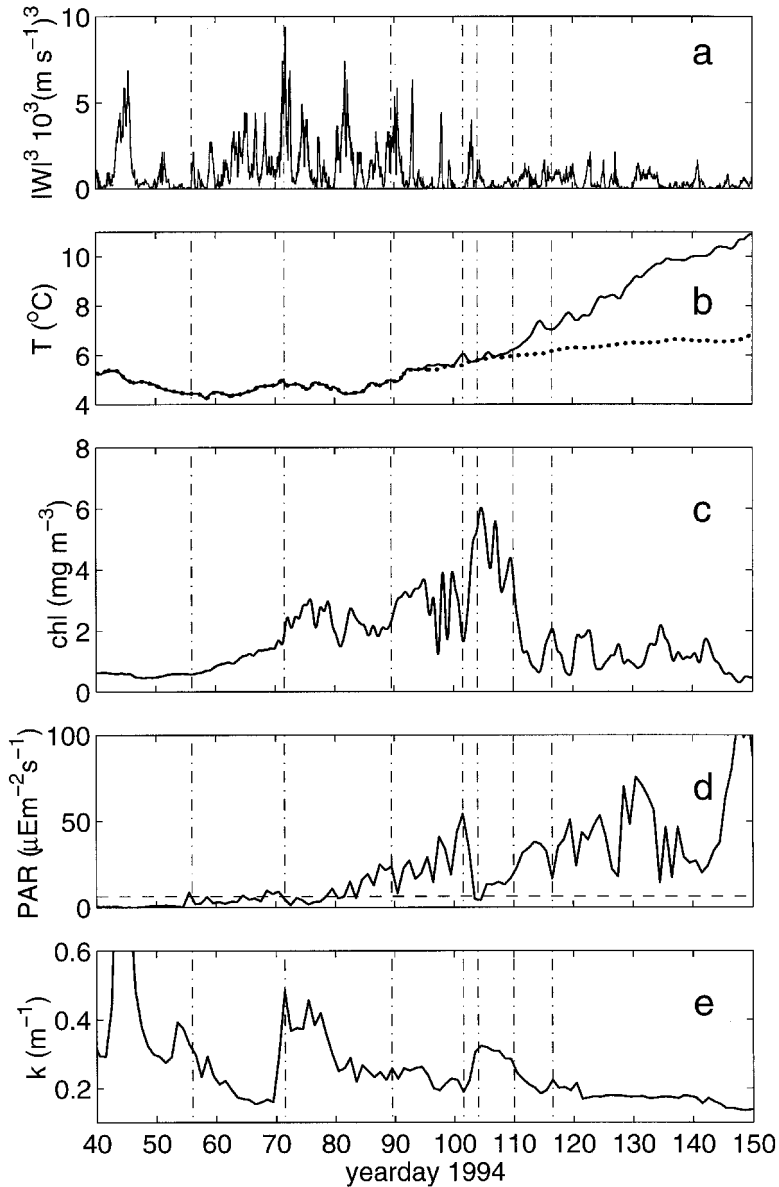


Figure 4. Low-pass filtered (\sim daily averaged) observations made at the INP mooring location during February–June 1994. (a) Wind speed cubed. (b) Water temperature at 2 m (solid line) and 43 m depth (dashed line). (c) Calibrated chlorophyll derived from fluorescence data at 11 m. (d) PAR at 11 m depth (solid line) and threshold level for growth (dashed line). (e) Irradiance attenuation coefficient determined from PAR measured above the surface and at 11 m depth, assuming an exponential decrease with depth.

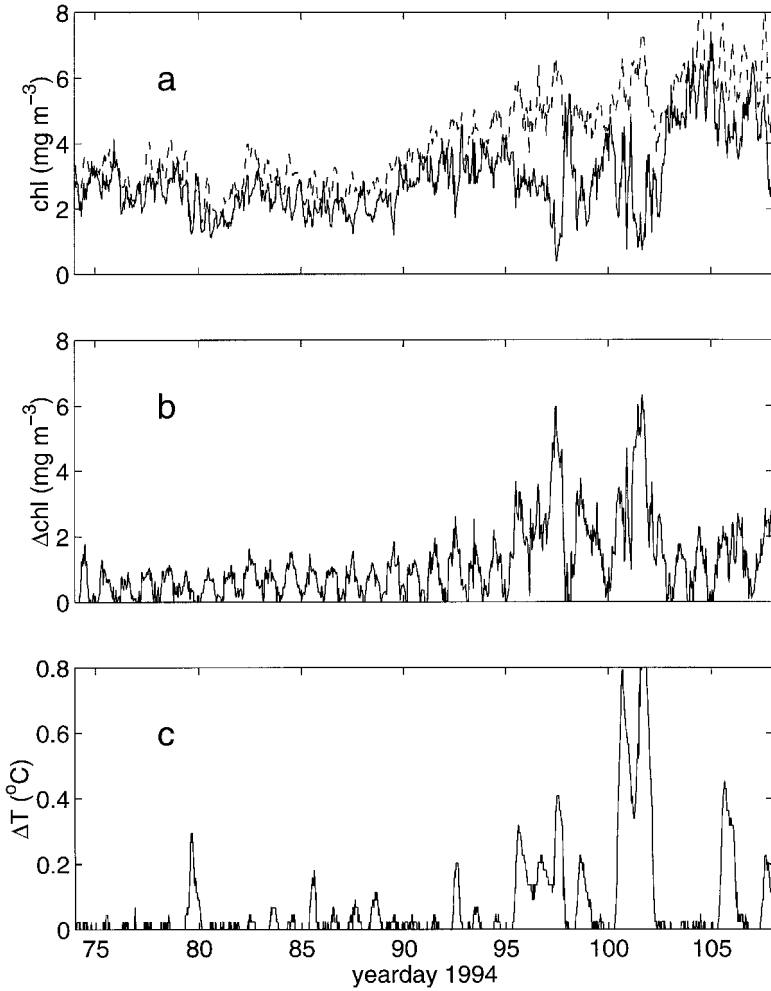


Figure 5. Differences between hourly sampled data at two depths. (a) Chlorophyll at 11 m (solid line) and 23 m (dashed line). (b) Chlorophyll at 23 m–11 m depth. (c) Temperature at 2 m–22 m depth.

North Sea (Gieskes and Kraay, 1984; Mills *et al.*, 1994) to about 1 mg m^{-3} . This end of the spring bloom at 11 m coincides with a relatively prolonged period of reduction in wind speed (and relatively weak free convection), and the onset of semi-permanent seasonal stratification from mid April (day 109) onward. This is in accordance with earlier reports on similar ocean areas (Gieskes and Kraay, 1984; Walsh *et al.*, 1988; Cushing, 1992) and noted earlier by Riley *et al.* (1949). The nutrient concentrations are relatively low and not limiting for growth somewhat earlier, as we observed (NO_3 , Si) levels of (0.5 ± 0.3 , 0.3 ± 0.2) and (0.9 ± 0.4 , no Si observations), similar for both sampling depths of 10 and

40 m, at days 101 and 109, respectively. In summary, the spring bloom lasted about 50 days in the central North Sea in 1994.

Three weekly water sampling confirms that large vertical differences in chlorophyll-*a* persist through spring (e.g. 0.4 and 29 mg m⁻³ at 5 and 40 m, respectively, at day 144.45) until the start of the summer. This confirms earlier observations from the central North Sea (Gieskes and Kraay, 1984; van Haren and Joordens, 1990). *Guinardia flaccida* continued to dominate the phytoplankton through May but primarily near the bottom. In late spring chlorophyll levels at 11 m showed occasional increases, which appear to be associated with increased levels of mixing (e.g. day 116 in Fig. 4). We elaborate in Section 4b.

The counter-intuitive observation of increasing chlorophyll levels at 11 m (e.g. around days 90 and 104) at decreasing, though not limiting, light intensities is explored further, firstly during the period when a second fluorometer was moored at 23 m, where PAR is insufficient for growth throughout the spring bloom period.

4. Details of the fluorescence observations

a. Comparison of fluorescence records at 11 and 23 m

Despite the light limitation at 23 m, the values of chlorophyll observed at this depth are on average equal to or *larger* than those at 11 m (Fig. 5), and must have been imported from above. The variability with time of the difference between the two records is strong, and markedly different from their average. The frequency spectrum of the chlorophyll difference between 11 and 23 m shows a significant peak at 1 cycle per day (cpd), which is not apparent in the spectrum of the average of the two observed time series (Fig. 6). This reflects the occurrence of a strong diurnal signal in both observed time series, but with a phase difference of 180° (Fig. 5). The average signal shows spectral elevations around the semi-diurnal tidal frequency, and, surprisingly almost equal in size, the inertial frequency (Fig. 6). Both frequencies dominate horizontal advection and appear less in the difference signal. At synoptic frequencies between 0.2–0.5 cpd, the difference signal shows a weak elevation at periods of about 2.5 days (0.4 cpd).

Examples of these slower variations with time, e.g. around days 96 and 101 when chlorophyll at 11 m decreases while chlorophyll at 23 m increases, coincide almost exactly with periods of short term stratification; i.e. during periods of reduced near-surface turbulence production and associated small mixing length scales (Fig. 5c). During such periods sinking is likely to dominate the rate of change of biomass. From the phase differences of varying chlorophyll concentration at the two depths, we estimate the sinking rate at about 50–200 m day⁻¹ (6–23 10⁻⁴ m s⁻¹) using only the left-hand side of (2), which suggests a bloom consisting (partially) of heavy or aggregated diatoms (Munk and Riley, 1952; Walsh *et al.*, 1988; Cushing, 1992), and consistent with our observed dominance of *Guinardia flaccida*.

It has been postulated (Smayda, 1970) that such sinking rates can be attained only by senescent algae, but our values comply well with the minimum value of 70 m day⁻¹, which was estimated by Passow (1991) for a healthy population during a spring bloom in a similar

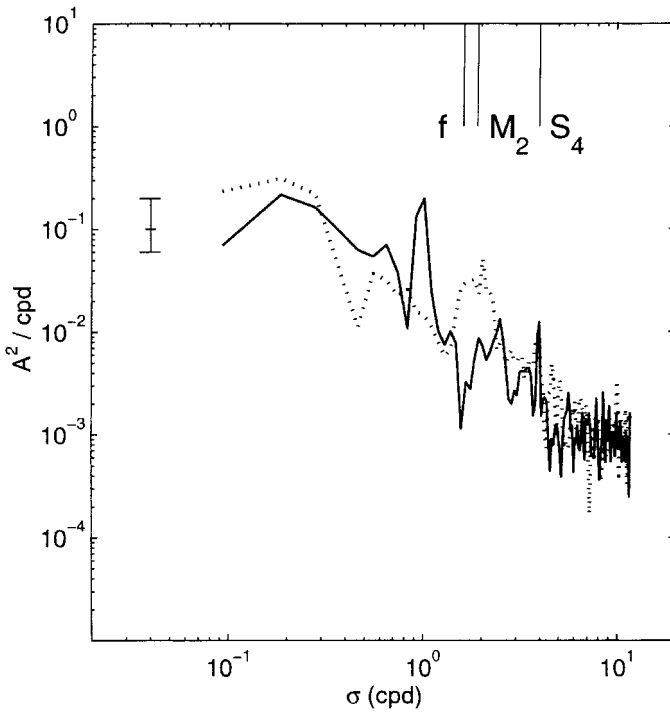


Figure 6. Amplitude squared spectra of the chlorophyll data in Figure 5, with the difference between data from 11 and 23 m (solid line) and the sum (= average \times 2) of the data from 11 and 23 m (dotted line). Some frequencies are given, the inertial frequency f , the dominating semi-diurnal lunar tide M_2 and the surprisingly strong (at 11 m only) fourth diurnal solar S_4 .

area (the Baltic) to ours. As the spring bloom progresses, the relative amount of sinking material increases, which may be attributed to the decreasing levels of turbulence following increased heat input, or to an increasing proportion of heavier phytoplankton species.

Shortly after turbulence regeneration near the surface, as inferred from the destruction of the short term stratification, the difference in chlorophyll levels at the two depths becomes negligible. It follows that the increase in chlorophyll at 11 m may not just be attributed to local growth, for which the near-surface layer is the source, but it is also due to resuspension of material that had either sunk earlier or that had grown deeper in the water.

Given the estimates of the sinking rate above and using simple scaling arguments for an advection-diffusion balance in (2), with a typical vertical length scale of 20 m, the associated vertical eddy diffusivity would amount to about $K \approx 1-4 \times 10^{-2} \text{ m}^2 \text{ s}^{-1}$ (and less when growth is occurring), which are realistic values for the bottom boundary layer in the North Sea (Veth, 1990), and which are the *lower* limit for atmospheric-free convection as observed by Brainerd and Gregg (1993) across the diurnal thermocline. Hence, this interpretation of the variation with time of chlorophyll due to alternating mixing and

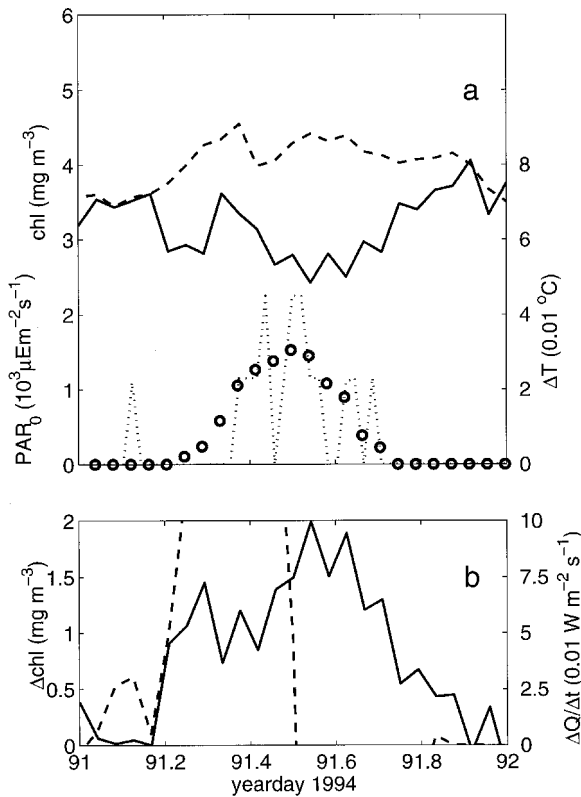


Figure 7. Typical example of one day of hourly sampled data. (a) Chlorophyll at 11 m (solid line) and 23 m (dashed line), PAR measured above the sea surface (circles) and temperature difference between 2 and 22 m depth (ΔT , dotted line). (b) Chlorophyll at 23 m–11 m depth (Δchl , solid line) and rate of variation with time of net radiation (dashed line).

sinking events may also be invoked to explain the strong diurnal cycle of the difference chlorophyll signal (Figs. 5 and 7).

Numerous observations have been made of a decrease in near-surface fluorescence during daytime (e.g. Lewis *et al.*, 1984; Denman and Gargett, 1988; Mills and Tett, 1990; Stramska and Dickey, 1992). Generally, this has been attributed to physiological effects, particularly photoinhibition of *in vivo* fluorescence following exposure to high levels of irradiance. It is questionable whether the maximum mid-day PAR levels of $\ll 250 \mu E m^{-2} s^{-1}$ would influence the fluorescence emission of phytoplankton. The fact that the reduction in chlorophyll concentration (fluorescence) at 11 m begins at or shortly before dawn further suggests that photoinhibition may be discounted (Fig. 7).

Similar shallow-sea observations have been made by Mills and Tett (1990). Although they do not elaborate, their data also show a near-surface fluorescence decrease starting at or just before dawn, and an increasing diurnal periodicity when the spring bloom

progresses. We note that in our data the daytime decreases in chlorophyll at 11 m are accompanied by more or less simultaneous increases at 23 m *and* increases in (small) vertical temperature differences.

Hence, the observed diurnal variability too seems attributable to variations in buoyant turbulent production, which may extend to about 40 m depth during night-time (Brainerd and Gregg, 1995), and is sufficient to reach the near-bottom mixing layer in our case. The observed asymmetry between fast sinking (~ 1 h between 11 and 23 m) and relatively slow mixing (~ 4 h) around sunset complies well with the direct turbulence measurements by Brainerd and Gregg (1995). An examination of their data (e.g. their Fig. 6) shows a weak decrease in turbulence intensity from its night-time maximum at about 1 h before sunrise, accompanied by, at times, small onsets of stratification near the surface. During such periods the surface heat flux started to decrease from its overnight maximum, although it was still positive.

Given the potentially fast sinking rate of heavy or aggregated phytoplankton, their vertical distribution may be expected to change quickly upon decreases in turbulence level. This may explain the rather instantaneous response of the chlorophyll level at 11 m upon the rate of change with time of net radiation $\Delta Q/\Delta t$, while Q is still negative (Fig. 7b). Apparently, variations in net radiation alone are sufficient to resemble decreasing turbulence levels in the near-surface layer, which may also be inferred from the data presented by Brainerd and Gregg (1995). For example the data shown in Figure 7 are qualitatively similar throughout the entire spring bloom period, but the time of the day when changes occur varies by ± 1 h, which may reflect variations in contributions from sensible and latent heat fluxes.

In general, the observations made later in spring show the same trends as above, except for details as will be discussed in Section 4c. Firstly, we compare the spring bloom fluorescence data with extracted chlorophyll-*a* data.

b. Extracted chlorophyll-a data

HPLC determined chlorophyll-*a* concentrations from water samples obtained during days 98 (on which samples were taken from surface to bottom, every 5 m), 101 and 109 generally support the detailed fluorescence observations. Chlorophyll-*a* levels from samples taken at 5 and 10 m depth did not differ significantly and describe the “near surface” values equally well. It is noted however, that all samples were taken during periods of relatively calm weather, and the largest values of chlorophyll-*a* were found closest to the bottom and not near the surface. On day 109, when the fluorometers were on board for servicing, hourly water sampling at three depths was performed during a 12-hour period (Fig. 8). With reference to the observed vertical temperature differences, the observed difference in chlorophyll-*a* levels between the two fluorometer depths is qualitatively similar to that observed with the fluorometers at day 107. This further supports our earlier conclusion that the fluorescence data are little affected by physiological (light) effects.

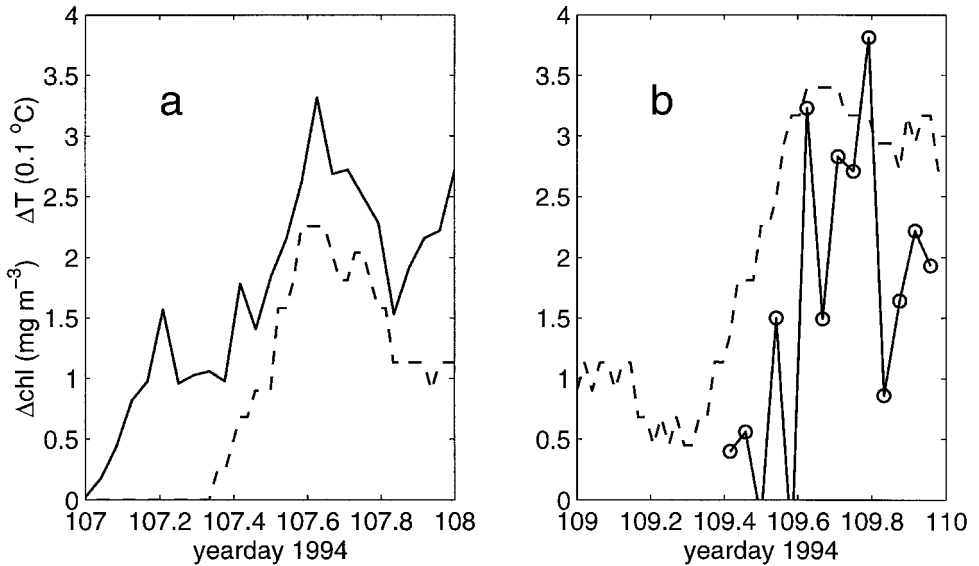


Figure 8. (a) Chlorophyll at 23 m–11 m depth from fluorometers (solid line). (b) Chlorophyll-*a* at 23 m–13 m depth by HPLC from water samples (circles and solid line). In both graphs the temperature difference between 2 m and 22 m depth is given by the dashed line. Note the nonoverlapping periods of sampling.

c. Fluorescence at 11 m during and after the spring bloom

The decrease in turbulence associated with the establishment of stable (seasonal) stratification from day 109 onwards (Fig. 9) appears to be responsible for the sinking of the bloom resulting in a decrease in near surface (11 m) fluorescence and a corresponding increase near the seabed. At our mooring site, the bloom persists in the turbulent near-bottom layer for some time (cf Section 3), which, as will be shown, occasionally induces an increase in near-surface chlorophyll.

As our fluorometer at 23 m depth failed after day 108, we compare here the fluorescence record from 11 m before and after the end of the spring bloom with temperature and radiation data. Generally, the established (seasonal) thermocline is located well below this fluorometer and varies in depth between 15 and 25 m, at the tidal and synoptic frequencies (Fig. 9). Gradually with time, the water column warms and occasionally during warming periods, the fluorometer is within short term near-surface stratification (e.g. around days 114 and 130). The warming periods are succeeded by periods of cooling as can be inferred from thermocline deepening (e.g. around days 121 and 131; Fig. 9a), which reflects erosion by atmospheric- (not just wind) induced mixing.

Such cooling periods of about 2 days duration are associated with increases in fluorescence at 11 m. In general, the near-surface fluorescence variations with time at these synoptic time scales correspond well with the varying stratification rate of the water column (shown by $-\Delta T$ in Fig. 10a). We note a relatively short time lag between the two

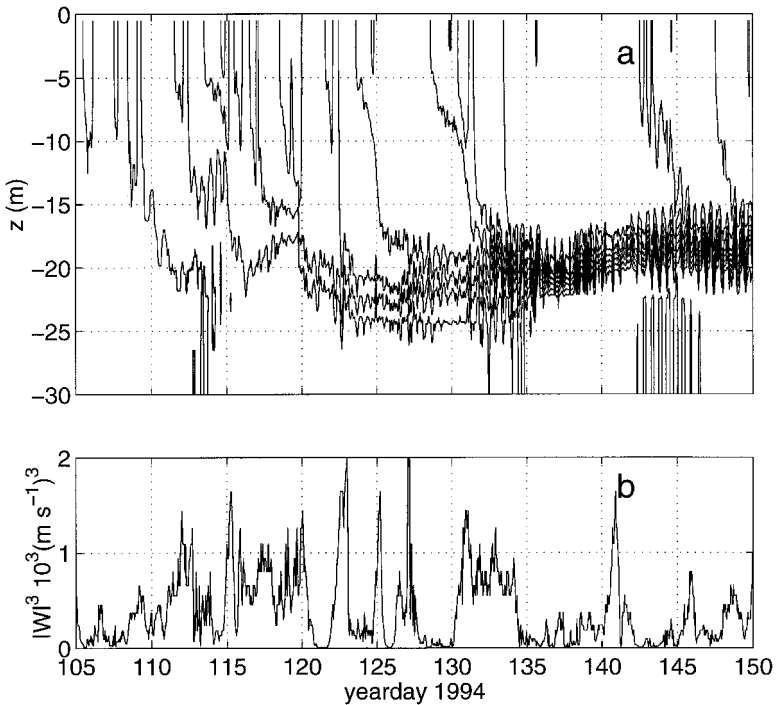


Figure 9. The spring stratification period (starting at day 109). (a) Isotherms between 6 and 11°C given every 0.5°C for the first 30 m depth as a function of time. (b) Wind speed cubed.

time series, which is on average 6 h, with fluorescence leading $-\Delta T$ until day 130, and less clear after that. Otherwise, this close correspondence is similar to the spring bloom period and, as before, we attribute the variations in fluorescence at 11 m to variations in mixing of phytoplankton from below, with the notion of a faster response of fluorescence upon mixing than the response of temperature (difference) upon mixing from above. We refer to Figure 4 to note that periods of fluorescence increase are accompanied by a decrease in local PAR.

The main difference in the fluorescence at 11 m and stratification rate data comparison between the spring bloom and stratified periods occurs at time scales of a day and shorter. During both observational periods fluorescence shows strong daily variations (Figs. 5a and 10b), but with more apparent noise (subday variability) during the spring bloom period (Fig. 11). During this period the daily varying part of the fluorescence signal shows reasonable correspondence in time with the daily varying temperature difference, except during the first four hours after sunrise (Figs. 11a and 11b). After the spring bloom, fluorescence at 11 m is even more dominated by a daily cycle, which now precedes $-\Delta T$ by on average 5 h (Figs. 10b and 11c), which is about the same time lag as inferred earlier for the synoptic time scales.

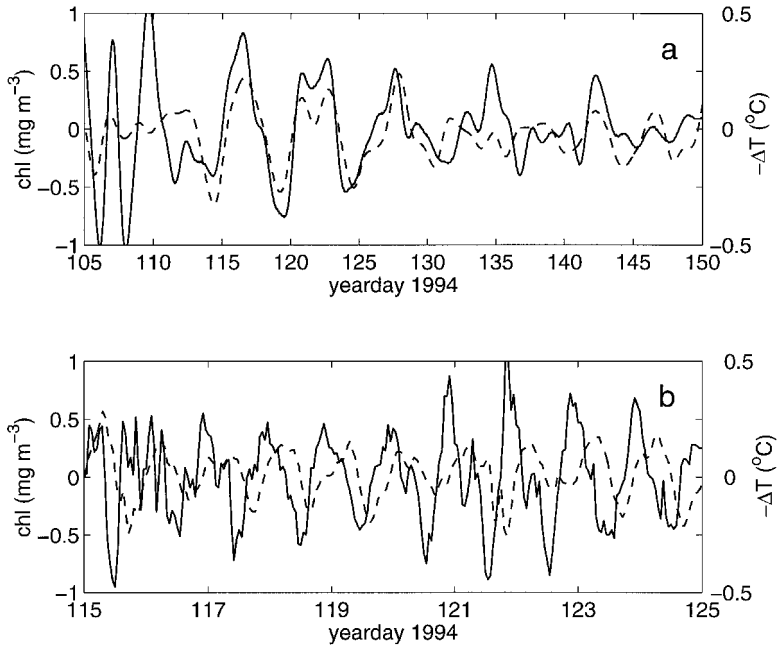


Figure 10. Comparison between chlorophyll at 11 m (solid lines) and the temperature difference between 2 and 43 m (ΔT , dashed lines) during the spring stratification period. (a) Band-pass filtered data with cut-off frequencies at about 0.8 and 0.15 cpd. (b) High-pass filtered data with the cut-off frequency at about 0.8 cpd.

The daily minimum in fluorescence at 11 m shifts forward around mid-day by about 2 h as compared to during the spring bloom, so that it even leads in time the observed change in net radiation ($-Q$), whereas the temperature difference becomes more related to the time integral of net radiation (cf. (1) and Fig. 11c), which explains the augmentation of the phase difference. Without further knowledge about the effects of mixing on heating and phytoplankton transport, this may indicate that, over time scales of a day, internal turbulence affects near-surface fluorescence after the spring bloom slightly and that physiological effects become more important. For example, local PAR increases by a factor of four within two months (Fig. 11) and E may become reduced.

A further source of physiologically induced variability could be the daily rhythm of cellular carbon/chlorophyll ratio (C/chl) (Owens *et al.*, 1980). Their observations (on the diatom *Thalassiosira gravida*) show a decrease in C/chl (mainly due to an increase in chlorophyll), approximately by a factor of two, and starting shortly before dawn to a minimum value three hours later, followed by a submaximum around mid-day and an increase, leading to the night-time maximum, which begins about 2 hours before sunset. Their observed daily pattern shows a striking similarity to our fluorescence observations during the early phase of the spring bloom (Fig. 11a), but, when entirely due to variations

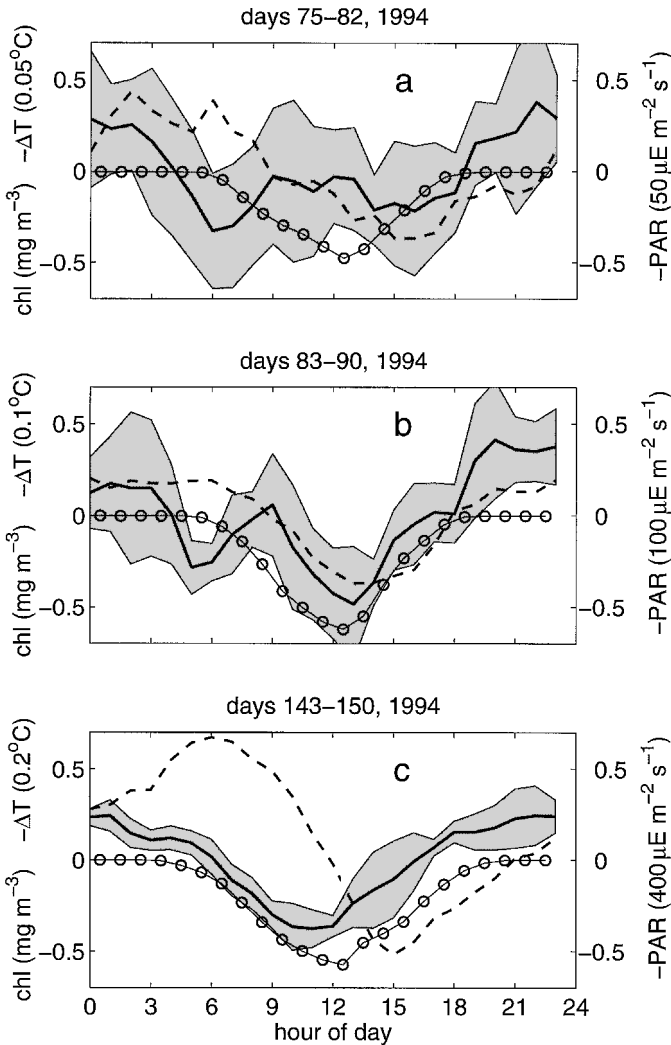


Figure 11. Comparison of typical daily variations during and after the spring bloom. Hourly data are given, averaged over 7 days. In all graphs chlorophyll at 11 m (thick solid line) is plotted in a shaded area of $\pm \sigma$ (one standard deviation) with $-\Delta T$ between 2 and 43 m depth (dashed line) and $-Q$ (circles). The data are arbitrarily offset along the vertical coordinate. Note the change in scale for ΔT and Q between the different graphs. (a) The early spring bloom period. (b) About the average of the spring bloom period. (c) Well into the spring stratification period.

in cellular chlorophyll content, it is exactly opposite in sign to our near-surface observations and merely mimicks our data from 23 m depth.

Thus, in an attempt to find alternative explanations for our fluorescence observations, some features remain puzzling. Firstly, can we explain the link between fluorescence and solar radiation, with fluorescence either responding very quickly to increasing irradiance

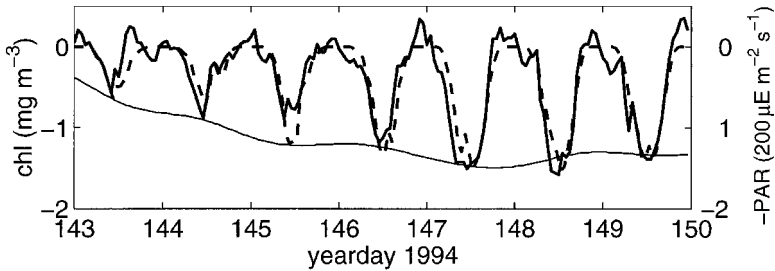


Figure 12. PAR (dashed line) and fluorescence at 11 m during the late spring stratification period. High-pass filtered chlorophyll (heavy solid line; cut-off frequency at 0.8 cpd) which is normalized by the corresponding low-pass filtered part of the signal (thin solid line; offset arbitrarily) and offset per day by the average night value.

(within 1 h; Fig. 11b) or even preceding its daily increase (Fig. 11c)? Secondly, given the close relationship between PAR and fluorescence over a wide range of values we question the apparent lack of threshold level for a reduction in the fluorescence emission coefficient in our data (Fig. 12). Thirdly, Owens *et al.* (1980) found the same daily variation in C/chl at 30 m depth as near the sea surface, whereas we find *opposing* variations in fluorescence at comparable depths.

5. Discussion

About half a century ago, Riley *et al.* (1949) reported that the combination of turbulent diffusion and sinking velocity needs to be considered in any model on the explanation of observed vertical profiles of phytoplankton distribution, whether observed in the ocean or in shallow seas (their Fig. 21). They inferred from their limited data sets, which were generally obtained in deeper waters than ours, typical spring bloom settling velocities of about $5\text{--}10\text{ m day}^{-1}$ with vertical turbulent diffusivity coefficients of about $K \approx 0.005\text{ m}^2\text{ s}^{-1}$. Although they did not give estimates of sinking velocities from all data obtained at their shallowest station, indications point at higher values than given above for Georges Bank (about 50 m water depth; $K \approx 0.02\text{ m}^2\text{ s}^{-1}$). They also stated that the near-surface phytoplankton concentrations found in the Sargasso Sea (“open ocean”) were comparable to the lowest values found in the data from near coastal areas and that most spring blooms occurred before the onset of stratification. Today, with the aid of modern electronics, we may be able to verify their findings on (much) shorter time scales.

The correspondence between fastly sampled variations of fluorescence and vertical temperature differences on time scales longer than a day has led us to a hypothesis similar to Riley *et al.*'s (1949) that near surface phytoplankton biomass, during the spring bloom in the Oyster Grounds, is primarily controlled by variations in turbulence levels coupled with “fast” sinking. Therefore, as turbulence levels exhibit a strong diurnal signal a matching response in the distribution of biomass is to be expected. Our data, however, do leave us with some questions regarding fluorescence variations at (sub-)day time scales.

One of the remaining questions addresses the complexity of the relationship between fluorescence and phytoplankton biomass (chlorophyll). If we ignore the observed (peculiar) difference in phase, the correspondence between fluorescence and local PAR, especially in late spring, seems to point at the often reported physiological effect of light, with mid-day fluorescence minima (Fig. 12). However, we did not find a clear threshold level above which this light induced decrease occurs but, we did find similar daily variations in extracted chlorophyll-*a* from water samples as in fluorescence and, we observed an opposite behavior of fluorescence at 23 m depth in early spring, with maxima around mid-day. Similarly, possible variations in the C/chl ratio do not offer a final explanation for the observed subday variations in near-surface fluorescence during the spring bloom.

As a result, it seems that fluorescence represents chlorophyll reasonably, but we note that we did not consider other possible factors in our analysis, such as varying nutrient levels, varying composition of phytoplankton species, self-propelled phytoplankton motion, which is unlikely for diatoms, and grazing, which is probably low in early spring. However, all these factors are unlikely to vary and be effective for phytoplankton concentrations on the short time scales as observed, and daily varying turbulence levels appear to explain, at least partly, the diurnal rhythm in near-surface fluorescence provided the following assumptions hold.

Firstly, daily varying turbulence levels are better represented by variations in solar (net) radiation than by vertical temperature differences, especially when a permanent stratification exists, as observed by Brainerd and Gregg (1993, 1995). Secondly, fluorescence responds much faster to variations in turbulence levels than temperature does, which rate of change is also governed by the surface (heat) flux and which time scale is relatively large due to the heat capacity of water. This is akin to the conclusions of Scully and Vincent (1997), who observed a closer relationship between solar radiation and vertical hydrogen peroxide differences than vertical temperature differences, from which they concluded that hydrogen peroxide responds more rapidly to mixing. We note that the generation of a clear daily cycle in marine snow is entirely governed by turbulence, and neither by growth nor grazing, as Ruiz (1997) concluded from numerical modeling analysis.

The relationship between daily varying solar radiation and near-surface fluorescence is also suggested by the spectral decomposition of their time series. In Figure 6 (and also Figs. 11a and b) we observe an elevation at a fourth daily frequency in (predominantly near-surface) fluorescence, albeit we note that the statistical uncertainties are large. Surprisingly, this spectral peak is not associated with the first harmonic (M_4 , period ≈ 6.21 h) of the dominant semi-diurnal lunar tide, which would point at bottom friction induced mixing events or at mooring motion (van Haren, 1996), but it shows up at an average period of 6.00 h, the period of the first harmonic of the semi-diurnal solar tide (S_4). Of all parameters we could test, only the net radiation (and PAR measured above the sea surface) show a spectral increase at the same frequency, although the spectral content relative to the one at 1 cpd was much less than for near-surface fluorescence.

It is unclear what drives this fourth daily solar cycle and why it is appearing relatively strong in the fluorescence record from the spring bloom. Here, we just note that direct turbulence measurements by Brainerd and Gregg (1995) also seem to show a fourth daily cycle (their Figs. 6 and 14), particularly clear during the night. If not related to a (variable with time) fourth daily cycle, the rather persistent submaximum in near-surface fluorescence observed around 9 o'clock of the day during the spring bloom and not later in spring, may point at growth, local in time. During the period between days 88–95 for instance, the average increase between 6–9 o'clock amounts $0.4 \pm 0.1 \text{ mg m}^{-3}$. If we hypothesize no further growth during the remainder of a day, the net growth over the period of a week would amount to 2.8 mg m^{-3} , which is about twice the total increase in chlorophyll over that period (1.6 mg m^{-3}).

6. Conclusions

We have found that data from fluorometers moored in shallow seas represent phytoplankton chlorophyll content variations well during the spring bloom, with little fouling when left unattended for periods up to a month. The relationship between chlorophyll and fluorescence is linear, but *in situ* calibrations remain necessary for comparison with extracted chlorophyll *a* from water samples. If, as we hypothesize, phytoplankton variations with time are mainly governed by turbulence variations, then we may have shown that of all (bulk) parameters we have measured, fluorescence constitutes the outstanding means to indicate turbulence variations. This has to be verified in the future by direct turbulence measurements.

We have shown that in shelf seas the spring bloom may occur prior to the onset of any stabilizing (seasonal) stratification, as indicated by Riley *et al.* (1949). This behavior contrasts with the classic view of phytoplankton growth and embraced in the critical depth hypothesis (Sverdrup, 1953). Although this contrast has been noted before (Townsend *et al.*, 1992, 1994) we do not attribute it to a reduction of turbulence, but to a coupling between the bottom and surface mixing layers; i.e. the photic and nutrient rich parts of the water column, and the associated “mixing” of algae. Thus, relatively fast sinking algae may grow without being irretrievably lost from the euphotic zone, as would occur in deeper waters, resulting in enhanced biomass and production as in near coastal waters, where bottom friction alone generates sufficient turbulence to keep the entire water column mixed.

Growth can only occur near the surface when sufficient turbulence is available by atmospheric forcing, or deeper in the water column when the near-bottom mixing layer reaches high enough, both at the expense of limited light levels but favoring nutrient supply. Possibly, growth may occur near the surface during small, most frequently early, periods of the day only. Consequently, in shallow seas phytoplankton cannot induce thermal stratification, as has been reported for the ocean (Stramska and Dickey, 1993), and does not contribute to global warming or cooling.

Our observations also suggest that a phytoplankton spring bloom in shallow seas may

not be well represented in visible light satellite images as they can only be obtained during the day and, generally, during calm weather periods, when phytoplankton sink deeper into the water column. During the entire spring period we found phytoplankton well mixed through the water column or increasing in concentration with depth, rather than maximal near the surface. The subtle interplay of increased levels of turbulent mixing and onsets of stratification may vary from year to year and may, therefore, have a major impact on the succession of phytoplankton.

Acknowledgments. We greatly appreciate the assistance of the crews of the R. V. *Pelagia* and the R. V. *Holland* during INP. We thank Hans Malschaert for the nutrient data, Bouwe Kuipers and Roel Riegman for additional sampling near our mooring site. Leo Maas, Wim van Raaphorst, Herman Ridderinkhof, Bouwe Kuipers, Willem Stolte, Sjeff Zimmerman and Roel Riegman provided internal review and advice. HvH was supported by a grant from the Netherlands Organization for the Advancement of Scientific Research, NWO. DKM was supported by the U.K. Ministry of Agriculture, Fisheries and Food. This is NIOZ publication no. 3267.

REFERENCES

- Brainerd, K. E. and M. C. Gregg. 1993. Diurnal restratification and turbulence in the oceanic surface mixed layer, 1. observations. *J. Geophys. Res.*, *98*, 22645–22656.
- . 1995. Surface mixing and mixing layer depths. *Deep-Sea Res.*, *42*, 1521–1543.
- Cloern, J. E. 1991. Tidal stirring and phytoplankton bloom dynamics in an estuary. *J. Mar. Res.*, *49*, 203–221.
- Cushing, D. H. 1992. The loss of diatoms in the spring bloom. *Phil. Trans. R. Soc. Lond.*, *335*, 237–246.
- Denman, K. L. and A. E. Gargett. 1988. Multiple thermoclines are barriers to vertical exchange in the subarctic Pacific during SUPER., May 1984. *J. Mar. Res.*, *46*, 77–103.
- Gieskes, W. W. C. and G. W. Kraay. 1984. Phytoplankton, its pigments, and primary production at a central North Sea station in May, July and September 1981. *Neth. J. Sea Res.*, *18*, 51–70.
- Healey, F. P. 1973. Inorganic nutrient uptake and deficiency in algae. *Crit. Rev. Microbiol.*, *3*, 69–113.
- Lewis, M. R., E. P. W. Horne, J. J. Cullen, N. S. Oakey and T. Platt. 1984. Turbulent motions may control phytoplankton photosynthesis in the upper ocean. *Nature*, *311*, 49–50.
- Maas, L. R. M. and J. J. M. van Haren. 1987. Observations on the vertical structure of tidal and inertial currents in the central North Sea. *J. Mar. Res.*, *45*, 293–318.
- Margalef, R. 1978. Life-forms of phytoplankton as survival alternatives in an unstable environment. *Ocean. Acta*, *1*, 493–509.
- Mills, D. K. and P. B. Tett. 1990. Use of a recording fluorometer for continuous measurement of phytoplankton concentration, in *Environmental and Pollution Measurement Sensors and Systems*, H. O. Nielsen, ed., *Proc. SPIE*, *1269*, 106–115.
- Mills, D. K., P. B. Tett and G. Novarino. 1994. The spring bloom in the southwestern North Sea in 1989. *Neth. J. Sea Res.*, *33*, 65–80.
- Munk, W. H. and G. A. Riley. 1952. Absorption of nutrients by aquatic plants. *J. Mar. Res.*, *11*, 215–240.
- Niiler, P. P. and E. B. Kraus. 1977. One-dimensional models of the upper ocean, in *Modelling and Prediction of the Upper Layers of the Ocean*, E. B. Kraus, ed., Pergamon Press, Oxford, 143–172.
- Owens, T. G., P. G. Falkowski and T. E. Whitledge. 1980. Diel periodicity in cellular chlorophyll content in marine diatoms. *Mar. Biol.*, *59*, 71–77.

- Passow, U. 1991. Species-specific sedimentation and sinking velocities of diatoms. *Mar. Biol.*, *108*, 449–455.
- Pingree, R. D. and D. K. Griffiths. 1978. Tidal fronts on the shelf seas around the British Isles. *J. Geophys. Res.*, *87*, 4615–4622.
- Pingree, R. D. and R. P. Harris. 1988. An *in vivo* fluorescence response in the Bay of Biscay in June. *J. Mar. Biol. Assoc. U.K.*, *68*, 519–529.
- Prézélin, B. B. and A. C. Ley. 1980. Photosynthesis and chlorophyll *a* fluorescence rhythms of marine phytoplankton. *Mar. Biol.*, *55*, 295–307.
- Riegman, R., B. R. Kuipers, A. A. M. Noordeloos and H. J. Witte. 1993. Size-differential control of phytoplankton and the structure of plankton communities. *Neth. J. Sea Res.*, *31*, 255–265.
- Riley, G. A., H. Stommel and D. F. Bumpus. 1949. Quantitative ecology of the plankton of the western North Atlantic. *Bull. Bing. Ocean. Coll.*, *12* (art. 3), 1–169.
- Ruardij, P., H. van Haren and H. Ridderinkhof. 1997. The impact of thermal stratification on phytoplankton and nutrient dynamics in shelf seas: a model study. *J. Sea Res.*, *38*, 311–331.
- Ruiz, J. 1997. What generates daily cycles of marine snow? *Deep-Sea Res.*, *44*, 1105–1126.
- Scully, N. M. and W. F. Vincent. 1997. Hydrogen peroxide: a natural tracer of stratification and mixing processes in subarctic lakes. *Arch. Hydrobiol.*, *139*, 1–15.
- Sharples, J. and P. Tett. 1994. Modelling the effect of physical variability on the midwater chlorophyll maximum. *J. Mar. Res.*, *52*, 219–238.
- Smayda, T. J. 1970. The suspension and sinking of phytoplankton in the sea. *Ocean. Mar. Biol. Ann. Rev.*, *8*, 353–414.
- Stramska, M. and T. D. Dickey. 1992. Variability of bio-optical properties of the upper ocean associated with diel cycles in phytoplankton population. *J. Geophys. Res.*, *97*, 17873–17887.
- 1993. Phytoplankton bloom and the vertical structure of the upper ocean. *J. Mar. Res.*, *51*, 819–842.
- Sverdrup, H. U. 1953. On conditions for the vernal blooming of phytoplankton. *J. Cons. Perm. Int. Explor. Mer*, *18*, 287–295.
- Taylor, A. H. and J. A. Stephens. 1993. Diurnal variations of convective mixing and the spring bloom of phytoplankton. *Deep-Sea Res.*, *40*, 389–408.
- Tennekes, H. and J. L. Lumley. 1972. *A First Course in Turbulence*, MIT Press, Cambridge U.K., 293 pp.
- Tett, P. 1990. The photic zone, *in* *Light and Life in the Sea*, P. J. Herring, A. K. Campbell, M. Whitfield and L. Maddock, eds., Cambridge Univ. Press, Cambridge, U.K., 59–87.
- Thorpe, S. A. 1977. Turbulence and mixing in a Scottish loch. *Phil. Trans. Roy. Soc. Lond. A*, *286*, 125–181.
- Townsend, D. W., L. M. Cammen, P. M. Holligan, D. E. Campbell and N. R. Pettigrew. 1994. Causes and consequences of variability in the timing of spring phytoplankton blooms. *Deep-Sea Res.*, *41*, 747–765.
- Townsend, D. W., M. D. Keller, M. E. Sieracki and S. G. Ackleson. 1992. Spring phytoplankton blooms in the absence of vertical water column stratification. *Nature*, *360*, 59–62.
- van Aken, H. M. 1986. The onset of seasonal stratification in shelf seas due to differential advection in the presence of a salinity gradient. *Cont. Shelf Res.*, *5*, 475–485.
- van Aken, H. M., G. J. F. van Heijst and L. R. M. Maas. 1987. Observations of fronts in the North Sea. *J. Mar. Res.*, *45*, 579–600.
- van Haren, H. 1996. Correcting false thermistor string data. *Cont. Shelf Res.*, *16*, 1871–1883.
- van Haren, J. J. M. and J. C. A. Joordens. 1990. Observations of physical and biological parameters at the transition between the southern and central North Sea. *Neth. J. Sea Res.*, *25*, 351–364.

- van Haren, J. J. M. and L. R. M. Maas. 1987. Temperature and current fluctuations due to tidal advection of a front. *Neth. J. Sea Res.*, 21, 79–94.
- Veth, C. 1990. Turbulence measurements in the tidally mixed Southern Bight of the North Sea. *Neth. J. Sea Res.*, 25, 301–330.
- Walsh, J. J., C. D. Wirick, L. J. Pietrafesa, T. E. Whitledge, F. E. Hoge and R. N. Swift. 1988. High-frequency sampling of the 1984 spring bloom within the mid-Atlantic Bight: synoptic shipboard, aircraft, and *in situ* perspectives of the SEEP-I experiment. *Cont. Shelf Res.*, 8, 529–563.
- Woods, J. D. and R. Onken. 1982. Diurnal variation and primary production in the ocean - preliminary results of a Lagrangian ensemble model. *J. Plankton Res.*, 4, 735–756.